Microstrip Patch Antenna Design and Performance Study for Biomedical Application

Anas Abdulbasit Masoud Elgheriani

Submitted to the
Institute of Graduate Studies and Research
in partial fulfillment of the requirements for the degree of

Master of Science
in
Electrical and Electronic Engineering

Eastern Mediterranean University
July 2020
Gazimağusa, North Cyprus

Approval of the Institute of Graduate Studies and Research

Prof. Dr. Ali Hakan Ulusoy
Director

I certify that this thesis satisfies all the requirements as a thesis for the degree of Master of Science in Electrical and Electronic Engineering.

Assoc. Prof. Dr. Rasime Uyguroğlu
Chair, Department of Electrical and Electronic Engineering

We certify that we have read this thesis and that in our opinion it is fully adequate in scope and quality as a thesis for the degree of Master of Science in Electrical and Electronic Engineering.

Prof. Dr. Sener Uysal
Supervisor

Examining Committee

1. Prof. Dr. Sener Uysal

2. Assoc. Prof. Dr. Mehmet Toycan

3. Assoc. Prof. Dr. Rasime Uyguroğlu

ABSTRACT

Early stage of tumor detection is important due to increased chance for recovery and saving patient's lives, therefore, many types of researches are going out to find more techniques or methods to be used for breast cancer detection in early stages. The aim of this thesis is to investigate the tumor location after designing a UWB antipodal Vivaldi antenna.

In this thesis, an antipodal Vivaldi antenna has been designed using copper for patch and ground layers and FR4 for the substrate layer. The antenna is operating over a band from 3.38 to 10GHz. Also the antenna parameters which are reflection coefficient (S11), directivity and radiation pattern are included in this study. Moreover, to optimize the antenna radiation direction and reduce the sidelobe leve, a Tapered Slot Edge (TSE) technique is applied and shows -18.8 dB and 6.58 dBi for side lobe level and directivity respectively at 5 GHz.

The Specific Absorption Rate (SAR) is the tool used to indicate the tumor location in the coordinate system (x, y, z) in this research. Tests have been done with CST microwave studio using a breast model built with a radius of 50mm. For simulation tumor radius was changed from 10mm, 7mm and 5mm respectively. Also the antenna location changed to 3 different places for reliability. The tumor location is approximated to the same coordinates of the maximum specific absorption rate (SAR) which is examined at 5GHz, 6GHz, 7GHz and 8GHz. Simulations successfully show the correct tumor location while the antenna is facing the tumor.

Keywords: Antipodal Vivaldi Antenna, Tapered Slot Edges (TSE), Specific Absorption Rate (SAR), Tumor Detection and Coordinates.

ÖZ

Tümör tedevisinde, hastaların hayatını kurtarabilmek için erken tanı çok önemlidir ve meme kanserinin erken teşhisi için çeşitli araştırmalar yapılmaktadır. Bu araştırmaların neticesinde erken tanıyı sağlayabilecek teknik veya methodlar geliştirilmektedir. Bu tezin amacı UWB antipodal Vivaldi anteni tasarlayarak tümörün hasta vücudundaki yerini tespit etmektir.

Bu tezde, patch ve yer katmanları için bakır, alt tabakalar için FR4 kullanılarak bir antipodal Vivaldi anteni tasarlanmıştır. Tasarlanan anten 3.38 GHz ile 10 GHz arasında çalışmaktadır. Ayrıca, yansıma katsayısı (S11), directivity, radiation pattern gibi anten parametreleri çalışmaya dahil edilmiştir. Antenin radyasyon yönünü optimize etmek ve yan lob levelini düşürmek için Tapared Slot Edges (TSE) tekniği kullanılmıştır ve yan lobda -18.8 dB ile 6.58 dBi gözlemlenmiş olup directivity 5 GHz olarak gösterilmiştir.

Bu çalışmada, tümör lokasyonunu koordinat sisteminde (x, y, z) göstermek için Specific Absorption Rate (SAR) yöntemi kullanılmıştır. Simülasyonlar CST microwave kullanılarak yapılmıştır ve göğüs modeli 50 mm yarı çapı olacak şekilde kurulmuştur. Simülasyonlar, tümörün yarı çapı 10 mm, 7 mm ve 5 mm seçilerek gerçekleştirilmiştir. Ayıca, güvenirlik açısından tümörün lokasyonu 3 farklı yere konuşlandırılmıştır. Tümör lokasyonları aynı maksimum SAR kordinatlarında seçilerek 5 GHz, 6 GHz, 7 GHz ve 8 GHz frekanslarında denenmiştir. Sonuç olarak, anten tümör ile karşılaşınca lokasyonları başarılı bir seşilde tespit edebilmiştir.

Anahtar Kelimeler: Antipodal Vivaldi Anteni, Tapered Slot Edges (TSE), Specific Absorption Rate (SAR), Tümör Tespiti and Koordinatlar.

DEDICATION

To My Family

Dr. Abdulbasit Elgheriani & Dr. Faiza kutrani

Ahmed, Mohammed, Aws and Amena.

ACKNOWLEDGMENT

I would like to start with a great thank to my supervisor Prof. Dr. Sener Uysal for his advices, contribution and valuable guidance about this topic, he has helped me with the difficulties that I faced during this research and without his insistence this work can't be completed successfully. My gratitude words also extended to thank Assoc. Prof. Dr. Rasime Uyguroğlu chair for our department and Prof. Dr. Hasan Demirel vice rector for their great support and guidance.

I would like to extend my gratitude to all members of the Electrical and Electronic Engineering department family, academic and administrative staffs.

Special thanks for my parents, my brothers and my lovely sister for their unlimited support, love and care. Finally my friends Aws Elgheriani, Ayob Sultan, Mohamed Swaid and Hussian Benamer who have made memorable and pleasant time during this journey in the lovely city of Famagusta.

TABLE OF CONTENTS

LIST OF TABELS

LIST OF FIGURES

LIST OF SYMBOLS AND ABBREVIATIONS

AVA	Antipodal Vivaldi Antenna
c	Speed of light
CST	Computer Simulation Technology
EM	Electromagnetic
FCC	Federal Communications Commission
fr	Resonant Frequency
FR-4	Flame Retardant 4
h	Height
IEEE	Institute of Electrical and Electronics Engineers
L	Length
TSA	Tapered-Slot Antenna
TSE	Tapered Slot Edge
SAM	SubMiniature version A
SAR	Specific Absorption Rate
SSL	Side lobe level
W	Width
UWB	Ultra-Wideband Antenna
VSWR	Voltage Standing Wave Ratio
Z	Impedance
εr	Relative permittivity
$\varepsilon reff$	Effective relative permittivity
$\lambda 0$	Free space wavelength
λg	Wavelength of propagation

Chapter 1

INTRODUCTION

1.1 Introduction

Breast cancer in women is the most frequently occurring type more than other cancers especially for older women over 40 years old. Statistically among 232,340 cases reported, 39,620 cases resulted in death and 64,640 cases are in Situ according to the American statistics made in 2013 which shows the high risk of breast cancer for women[1].

Table 1.1: Estimated New Female Breast Cancer Cases and Deaths by Age, US, 2013 [1].

Age (Yrs)	Invasive Cases	Deaths	In Situ Cases
< 40	10,980	1,020	1,900
< 50	48,910	4,780	15,650
50-64	84,210	11,970	26,770
65+	99,220	22,870	22,220
All ages	232,340	39,620	64,640

In the last decade, Magnetic Resonance Imaging (MRI), Mammography and Ultrasound are the three main currently used technologies for diagnosing and detecting the tumor but mostly they still suffer from limitations [2].

Developing antenna designs for defense and medical applications are widely considered from researchers to reach ultra-wideband antenna with high efficiency and with the best accuracy as possible [3]. Antennas which are operating over the frequency spectrum from 3.1 to 10.6 GHz known as UWB based on the standards of

Federal Communications Commission (FCC) stated in 2004; moreover, the antenna size and weight are important features for the design [4].

The proposed antenna for this study is selected to meet the UWB characteristics since the Antipodal Vivaldi Antenna (AVA) is classified as end-fire travelling wave antenna that has a low side lobe level and wide beam width moreover it has high gain and directivity.

In this proposed design the copper and FR4 are used for conductor and substrate material respectively to reduce the cost of production.

1.2 Thesis Objectives

The thesis objective and the main goal for this study is to design an UWB antenna considering the performance target and material constraints and to study the antenna's gain, reflection coefficient, directivity and radiation pattern; parameter optimization also considered to reach the targeted performance.

Moreover, the differences in dielectric properties for the normal tissues compared to the malignant tissues are the base for the proposed method that has been used for this study and will be mentioned later in Chapter 5. Due to these differences, the absorption of electric field in malignant tissues is higher than the normal tissues which is used in the investigation of tumor location.

1.3 Thesis Overview

Thesis in general is divided into 6 chapters starting from the general view explained in the first chapter. Chapter 2 includes the main theory about the technology of microsrtip antenna design. In Chapter 3 the chosen antenna type for this study which is the Vivaldi

antenna is discussed in more detail. Chapter 4 includes the electric study for human breast tissue and Screening Methods for Breast Cancer. Chapter 5 presents the design and the simulation results of high performance Vivaldi antenna and its parameter study; also the SAR results, as a tool, are used to find tumor location in this chapter.

Chapter 2

THE TECHNOLOGY OF MICROSTRIP AND ULTRA WIDE BAND

2.1 Microstrip Antennas and Printed Circuits

For electrical and electronics applications when it comes to mass production the technology of printed circuits has been chosen due to their low cost and time consumption to fabricate. The technology of microstrip patch antennas are recognized as a printed circuit technology [5]. In 1970's the first printed, or microstrip patch antenna was designed and fabricated [6]. From that time challenge of having a low cost and profile antenna that meets the new life modern devices was the main topic for years of research.

The microstrip patch antenna has 3 layers as illustrated in Figure (2.1), the ground layer at the bottom, the dielectric substrate layer, and on top of the substrate is the radiator layer [7]. However, the radiator called the patch and the ground are both must be metallic. The patch can take different shapes but for simple analyses of antenna performance it is always chosen to be homogeny, Figure (2.2) shows some different shapes of the patch.

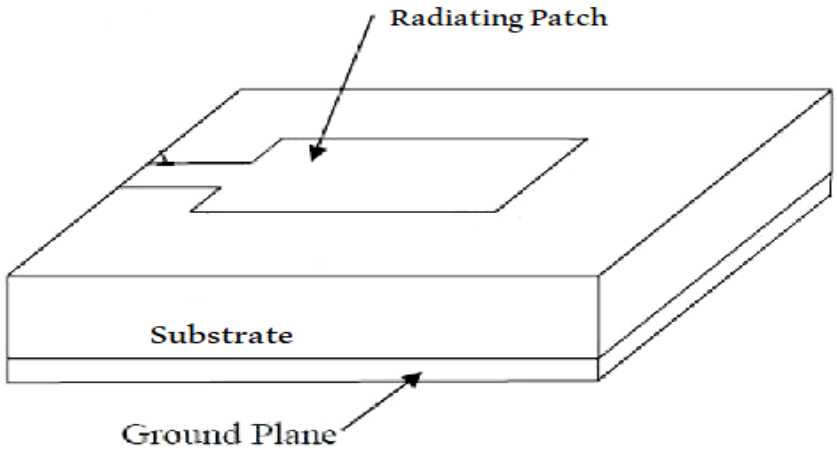

Figure 2.1: Microstrip Antenna Basic Structure

The microstrip antenna can be operated in a wide frequency range from 100MHz to 100GHz approximately [8]. However, comparing with other types of antennas, microstrip antenna suffers from lower gain, smaller bandwidth as well as low efficiency.

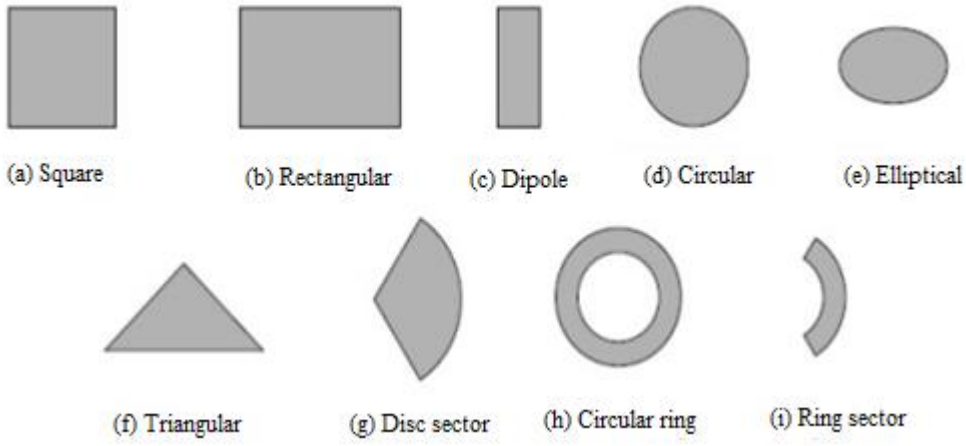

Figure 2.2: Patch Shapes

Antenna patch, matching network and feeding method should be properly designed to come up with a successful operating antenna as represented in Figure 2.3.

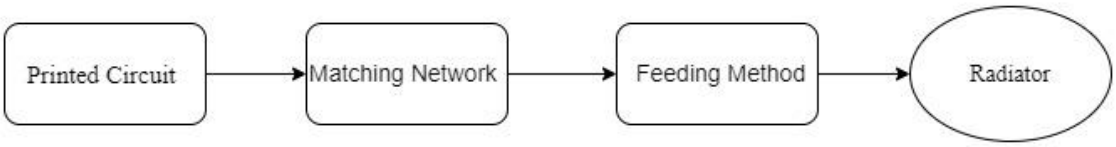

Figure 2.3: General Block Diagram to Design Microstrip Antenna

2.2 Antenna Parameters

The fundamental parameters to be studied for antennas are gain, return loss, input impedance and directivity.

2.2.1 Gain

By definition the antenna ability to radiate the changed form of input power in terms of radio waves in case of transmitting and the reverse in the receiving case the radio wave is converted into electrical power [9].

2.2.2 Return Loss

The power lost from the signal which is reflected or returned during the telecommunicating process is called the return loss and is calculated as a ratio in decibels:

$$RL(dB) = 10log_{10}\left(\frac{Pi}{Pr}\right) \quad (2.1)$$

Where P_i is incident power and P_r is the reflected power.

2.2.3 Voltage Standing Wave Ratio (VSWR)

VSWR is a measure of the reflected power on a transmission line and it is a function of the reflection coefficient its calculated by equation 2.2, if the VSWR of 1:1 means that there is no power being reflected back to the source.

$$VSWR = \frac{1+\Gamma}{1-\Gamma} \quad (2.2)$$

2.2.4 Radiation Pattern

Radiation pattern is a relation between the radiated power and distance away from the antenna. Antennas have varied shapes of radiation patterns based on the application

and the direction of communication needed. The main lobe where the radiation is maximal shows in which direction the antenna is radiating [10].

2.3 Feeding Techniques for Microstrip Antenna

Energy coupling to the radiator part of the antenna is called feeding, this feeding can be done in different ways based on the designer and the system requirements. The feeding techniques can be generally separated into two categories as non- contacting and contacting feeds. Strip and microstrip lines and coaxial cable all are methods to feed the microstrip patch antenna and they are the most commonly used methods. Using microstrip line for feeding the antenna can be applied in two different ways either both the line and the patch are on the same layer this is called co-planar coupling and it can be a direct or gap coupling as shown in Figure 2.4 or the line is on another layer.

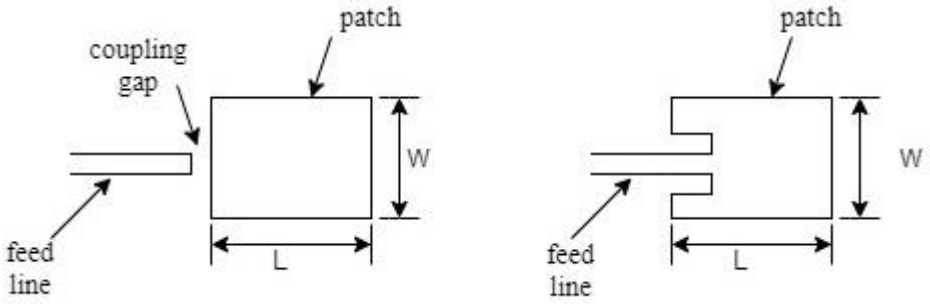

Figure 2.4: Co-planar Coupling

Proximity coupling and aperture coupling are used when the feed line is on another layer; both methods are shown in Figure 2.5 and 2.6 respectively. The selected method depends on the application requirements, for example, aperture coupling has the lowest spurious radiation and narrow bandwidth [10]; however, the other one has wide bandwidth as advantage.

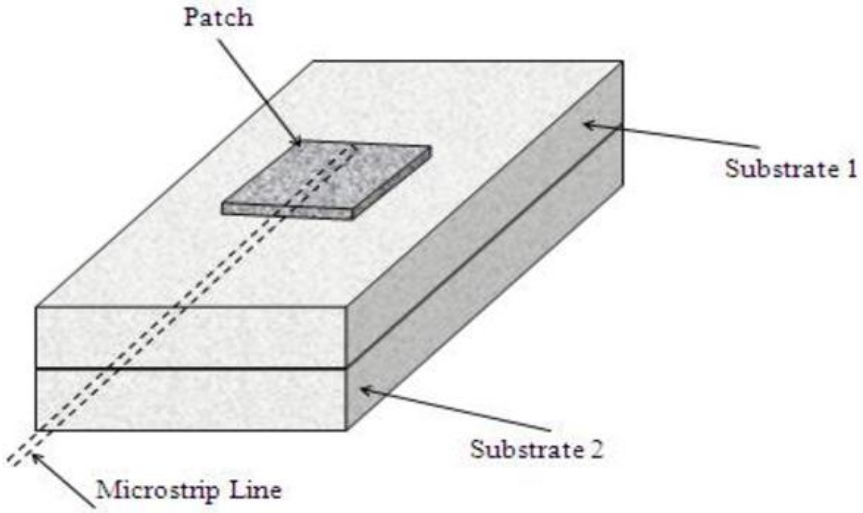

Figure 2.5: Proximity Coupling [9]

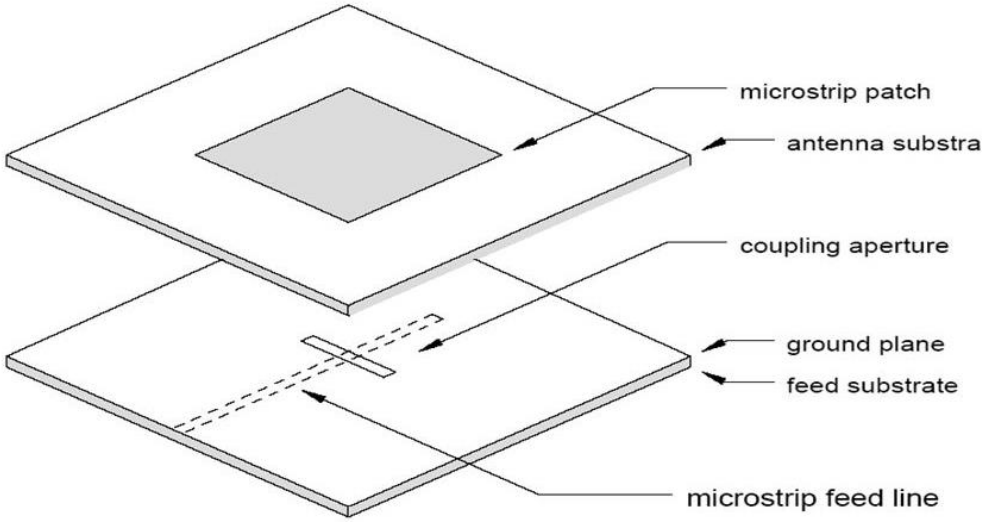

Figure 2.6: Aperture Coupling [9]

2.4 The Ultra Wide Band Technology

Frequency spectrum from 3.1 to 10.6 GHz is the frequency band for the UWB based on the Federal Communications Commission (FCC) regulation and it has a low power spectrum density (-41.3 dBm/MHz) to avoid the interference with the other narrow-band technologies operate in the same frequency band. The power spectral density is the average power in the signal per unit bandwidth and hence provides important information on the distribution of power over the RF spectrum. Figure 5.7 shows the

UWB spectral power density mask limited to –41.3 dBm by FCC to ensure that the UWB emission levels exceedingly small.

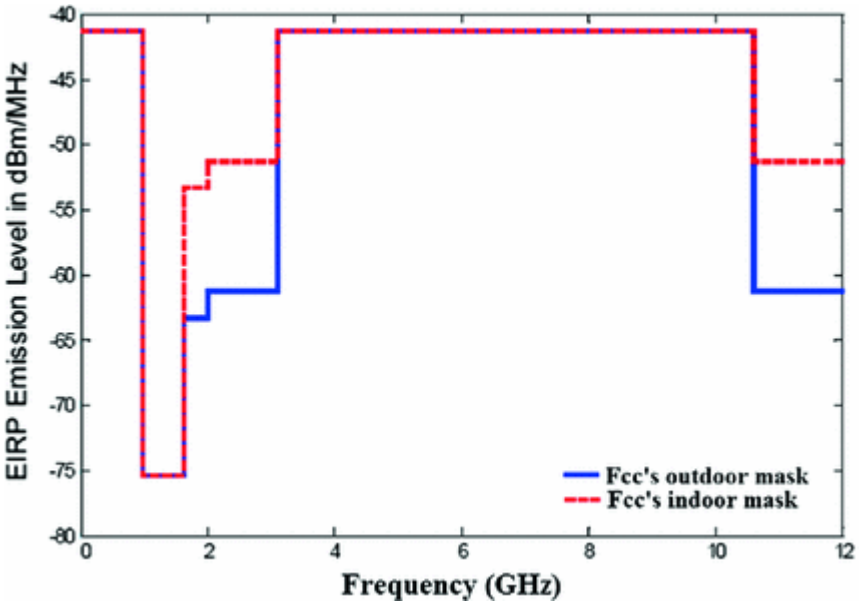

Figure 2.7: The UWB Spectral Power Density Mask

2.4.1 Application of UWB Technology

UWB waveforms have some unique properties and they are considered as short time duration [9]. UWB technology offer major enhancements in three wireless application areas: communications, radar and positioning or ranging.

2.4.1.1 Communication Systems

The exceptionally large available bandwidth is used as the basis for a short-range wireless local area network with data rates approaching gigabits per second. This bandwidth is available at relatively low frequencies thus the attenuation due to building materials is significantly lower for UWB transmissions than for millimeter wave high bandwidth solutions. By operating at lower frequencies, path losses are minimized and the required emitted power is also reduced to achieve better performance.

2.4.1.2 Radar Systems

For radar applications, these short pulses provide very fine range resolution and precision distance and positioning measurement capabilities. The very large bandwidth translates into superb radar resolution, which has the ability to differentiate between closely spaced targets. Other advantages of UWB short pulses are immunity to passive interference (rain, fog, clutter, aerosols, etc) and ability to detect very slowly moving or stationary targets [11].

2.4.1.3 Positioning Systems

For Global Positioning Satellite System (GPS), location and positioning require the use of time to resolve signals that allow position determination to within ten of meters. Greater accuracy is enhanced with special techniques used. Since there is a direct relationship between bandwidth and precision, therefore increasing bandwidth will also increase positional measurement precision.

Chapter 3

VIVALDI ANTENNA

Peter Gibson introduced and characterized a Vivaldi antenna for the first time in 1979 [12]. That antenna has been used in many applications, for example, radars, microwave imaging and wireless communication. The name of the antenna refers to Mr. Antonio Vivaldi who was a musician and he introduced a new musical device which Gibson gave to much weightiness and named his antenna design by this name[12].

3.1 Antenna Characteristics

Vivaldi antenna in one of Tapered-Slot Antenna (TSA) types ad it is represented in Figure (3.1) [13]. It is also classified under aperiodic traveling antenna where EM waves move to a slot that has been a part in the design. The design is comprised of a tapered slot shown in Figure 3.1 where the curved exponential W_A and W_E affects the beam width of the antenna [14]. The design can be done with a dielectric substrate or without. The importance of the antenna is based on end-fire beam that produced with low side lobes and appropriate gain and directivity; also it works over a large frequency bandwidth and is lightweight.

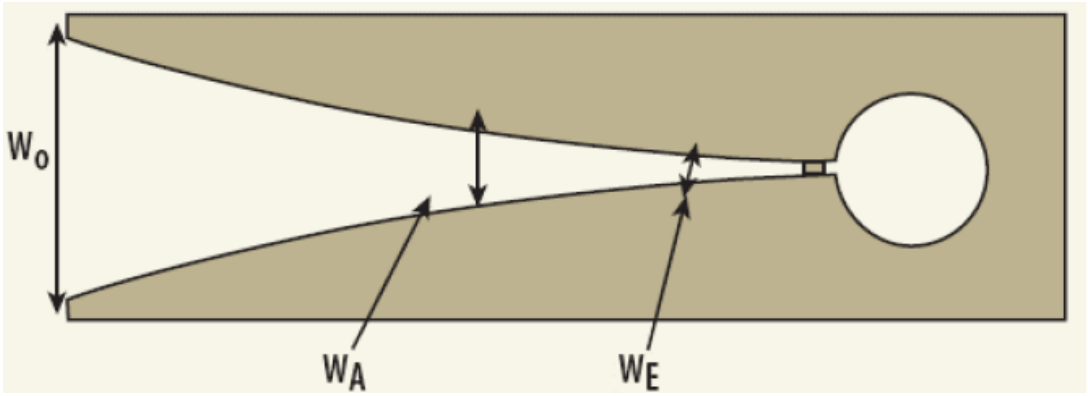

Figure 3.1: Tapered-Slot Antenna (TSA)

3.1.1 Antenna Operating Principle

As it mentioned previously, the Vivaldi antenna is classified as a surface-type traveling-wave antenna because the waves move along the antenna curved path. The space between the conductors and the substrate material affect the antenna radiation. For high radiation substrates with a low-dielectric constant materials are used.

The radiating section of the antenna is the end, wider part of slotline where the antenna couples the EM waves out of the structure and the radiation of EM waves characterized by end-fire direction [15]. The second parameter related to the operation of the antenna is the propagation section represented in Figure (3.2).

3.2 Types of Antennas

Radiation slot and slotline fedding are the two common features for planar tapered slot antennas. However, the difference in types exists for the shape of the slot only and it is illustrated in Figure 3.3. Different planar designs can be fabricated and a balanced slotline is used to feed the antenna and its impedance matching is effecting with the substrate dielectric constant.

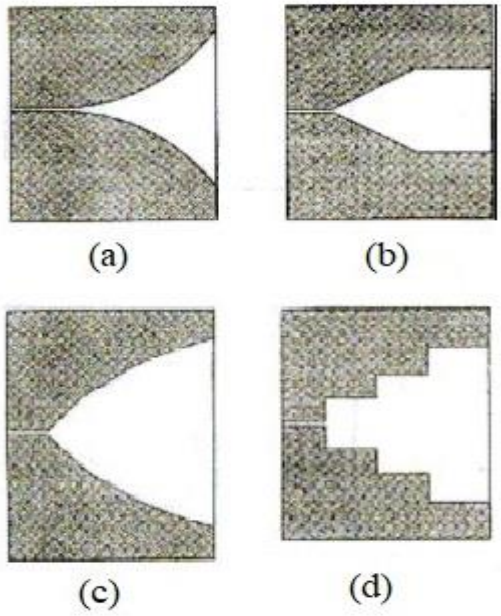

Figure 3.2: Different Types of Tapered-Slot Antenna: (a) Exponential, (b) Linear-constant, (c) Parabolic, (d) Step-constant [14].

3.3 Feeding Methods

It is important and essential to choose a proper feeding design to move the power from transmission line into the antenna with as less reflection as possible also to maximize the bandwidth because the high frequency limit is controlled by the feeder while the low frequency limit is controlled by the aperture size.

Microstrip transmission medium is mostly used in microwave integrated circuits (MICs) and a transition is necessary to couple microwave signals from microstrip circuit to the antenna, Figure (3.4) shows some feeding techniques.

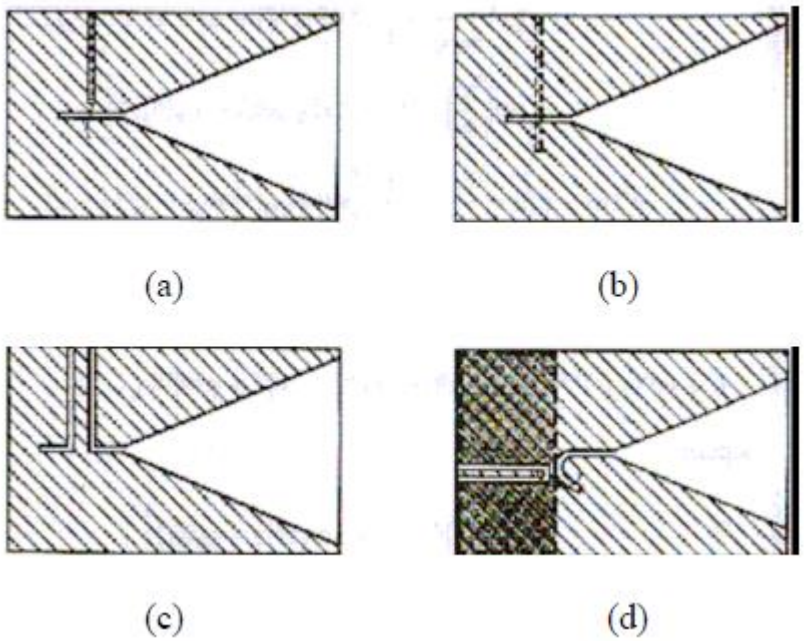

Figure 3.3: Different Feed Techniques: (a) Coaxial Line, (b) Microstrip, (c) CPW, (d) GCPW [14].

3.3.1 Microstrip Transition

In MICs the microstrip medium is commonly used as it is stated before. In this method a microstrip transmission line is used across the slot on the opposite side of the substrate. To have a design with less reflections a matching circuit between the slot line and the microstrip line should be used [17].

3.3.2 Coaxial Transition

A field coupling across the slot can be generated using coaxial feed line which is placed at the end of an open circuited slot [18]. It consists of an inner conductor and outer conductor where one side of the slot which is the ground plane is connected electrically with the outer conductor of the coaxial line; however, low characteristic impedance is an issue to design and for better matching a double-clad is used instead of single-clad; this decreases the slotline characteristic impedance which makes it possible to use a coaxial line.

3.3.3 Antipodal Slotline

The antipodal slotline referred to paired symmetric slotline strip and was first suggested by Gazit [19]. A parallel stripline is the transition region seen in Figure 3.5 and this transition type has an input feed which is microstrip. The slotline controls the radiation section in this design and the slot hole is avoided.

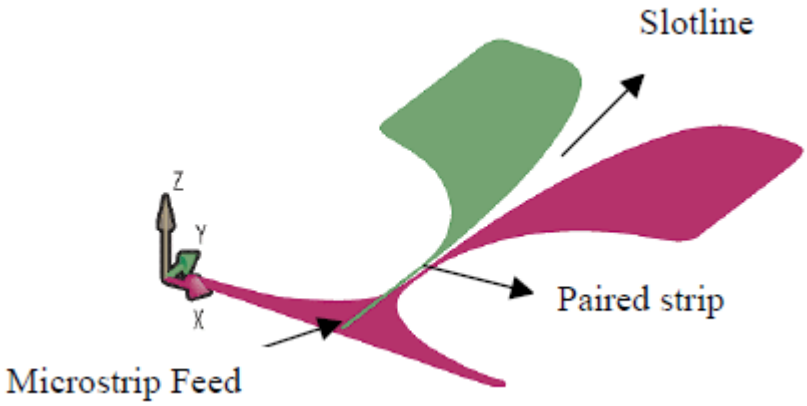

Figure 3.4: Antipodal Vivaldi Antenna [20].

A wide frequency band is realized in [20] after they used this method in their design. This design, however, has a weak cross-polarization performance; to avoid this an additional layer of dielectric material is added so the E-field distribution is balanced.

3.4 Tapered Slot Edges Method (TSE)

This method works to inhibited the edge current in order to increase the sidelobe level inhibited edge currents, which would promote the emergence of side lobes, acting as a resonator. Therefore, by removing edge currents, there is a relevant attenuation on the SLL of the AVA.

3.5 Substrate Material

The choice of dielectric substrate plays an important role in the design and simulation of transmission lines as well as antennas. Some important dimensions of the dielectric substrate are the dielectric constant, the dielectric loss tangent that sets, the dielectric

loss, the thermal expansion and conductivity and the cost and manufacturability. Dielectric constant and substrate thickness are the parameters determining the performance and radiation pattern, that is beamwidth, sidelobe level and gain of the antenna. Higher dielectric constant substrates give the advantage of smaller antenna dimensions for same performance. However, a more efficient design and a wider bandwidth is possible with low dielectric constant substrates. Low dielectric constant substrates also lower the scattering along the antenna and consequently spurious fields. Thus, the second parameter, tangent loss, shall also be considered to cope with this trade-off. Among the substrates with dielectric constant in the range of 2.2 to 10.2, FR-4 has a dielectric constant of ε_r = 4.3. FR-4 is chosen as the substrate material to be used in this work.

Chapter 4

COMPUTATIONAL ELECTROMAGNETICS AND SCREENING METHODS FOR BREAST CANCER

4.1 Computational Electromagnetics

Computational electromagnetics (CEM) is applied to model the interaction of electromagnetic fields with the objects like antenna, waveguides, aircraft and their environment using Maxwell equations.

The CEM techniques came into limelight after the introduction of three pillars of numerical analysis viz. FDTD (Finite Difference Time Domain), FEM (Finite Element Method) and MOM (Method of moments).

Commercial software codes have certain limitations, Agilent ADS could not model 3D structures, HFSS is accurate but execution time is high, WIPL-D does not support modeling Inhomogeneous dielectrics embedded metal objects and periodic structures. IE3D is not suited for geometry with finite details. However, for regular shapes like rectangular patch MOM based IE3D provides accurate results than FEM based IE3D. The complicated structures are dealt with accuracy by using CST Microwave Studio and HFSS. Although CST and HFSS has similar interface in dealing with geometry with fine details, CST had edge over HFSS software as it starts in time domain and ends in frequency domain.

4.2 Definition of Breast Cancer

Breast cells that have developed into a malignant tumor causes the breast cancer and the surrounding tissues is invaded by the cancer cells [21].

Women in their twenties are in low risk of the disease while this risk slightly rises at the age of forty-fifty and dramatically rises after fifty, as it is recorded in [21]; women older than sixty-five make fifty percent of the infected cases. Doctors are trying to bound the risk of infection by early diagnosis of the tumor. This increases the chance and the response to the treatment to kill the tumor. The major factors of developing cancerous breast tumors are [21]:

- Age:

  As the woman gets older the chance of getting breast cancer is increased.

- Weight:

  Overweight women have a higher risk of developing breast cancer.

- Abortion:

  Research shows that young women having abortion have a huge risk for the cancer.

- Inheritance:

  Existence or a history of breast cancer in close relatives play a major role for developing breast cancer.

4.3 Electrical Properties of Breast Tissue

When the EM microwaves propagates through the human body a change in the wave's amplitude occurs because of the body tissues. Fifty years ago the studies about the human body dielectric properties have started in a wide frequency band [22, 23] and those properties can be represented in two parameters as conductivity and relative

permittivity. However, the permeability of human body tissues is usually set as free space because tissue materials are nonmagnetic [22].

Wide range of research studies related to the permittivity and conductivity have been made. Generally, attenuation and reflection are the two main features that the EM waves are suffering from as they propagate through different body tissues because the attenuation is proportional to the conductivity. On the other hand, the amount of microwave energy stored is indicated by the permittivity also it showed the relation between the water content and the permittivity. For instance, the fat tissue has a lower water content and lower permittivity as well [24].

4.4 Most common Screening techniques

X-ray Mammography, MRI and Ultra-Sound are the methods that have been used to diagnose the breast cancer [25], [26]. For early detection of breast cancer and women with no symptoms of the disease an X-ray Mammography is used first for diagnoses. In the case an abnormal tissue is found then an ultrasound is carried out.

Sometime a medical biopsy is used when the signs of breast cancer information couldn't be produced using the mentioned methods and this biopsy is to find out whether the removed test sample tissue from the breast is healthy or cancerous.

X-ray mammography is harmful for the human because it is using an ionizing radiation. This technique records the movement through the breast also the breast is compressed in the medial between two plastic plates and that is causes pain for the patients [25].

Furthermore, Magnetic Resonance Imaging (MRI) using a high frequency and powerful magnified waves for constructing the image is also able to classify the soft tissue. However, it is need to be placed in specific shielded room and protected to limit the radiation of waves and avoid interference, this technique is time consuming and takes much time to check one patient.

Ultrasonic waves are used for Ultrasound imaging system to diagnose the state of the tissues as cancerous or not. This technique has a flexible cable which allows imaging from different angles.

Chapter 5

DESIGN AND SIMULATION RESULTS

This chapter illustrates the design process and parameter study for Antipodal Vivaldi Antenna; the simulated performance is investigated with CST STUDIO SUIT.

5.1 Antenna Geometry

Referring back to what discussed in Chapter 1, the UWB antenna should be simple in structure and compact and its gain is high in parallel with the wideband frequency. The antipodal Vivaldi antenna consists of three layers as mentioned before two radiation parts each one is lying on a different sides of the substrate. The radiation parts are symmetric and in general the radiation part has two edges (inner and outer) as an exponential line as it is illustrated in Figure 5.1; the EM wave radiation starts to operate as the separation distance between the conductors is increased.

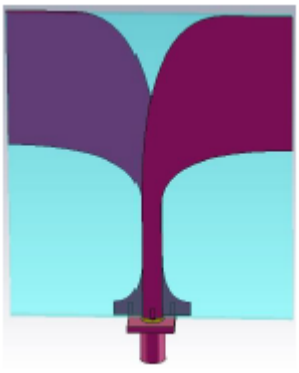

Figure 5.1: The Structure of Antipodal Vivaldi Antenna

The aperture slot width of the antipodal Vivaldi antenna is inversely proportional to the dielectric constant. Equation 5.1 shows this relation and the inner and outer exponential lines can be determined using equation 5.2.

$$W = \frac{c}{2f_{min}\sqrt{\varepsilon}} \tag{5.1}$$

Where W is the aperture slot width, f_{min} is the lowest frequency and ε is the dielectric constant.

$$y = c_1\, e^{qx} + c_2 \tag{5.2}$$

Where c_1 and c_2 are determined by the coordinates of the first and last points of the exponential line. q is the opening rate [24].

Microstrip line width is controlling the impedance matching and the operating frequency band performance is affected due to the change in the ground plane size, antenna width and q rate in equation 5.2.

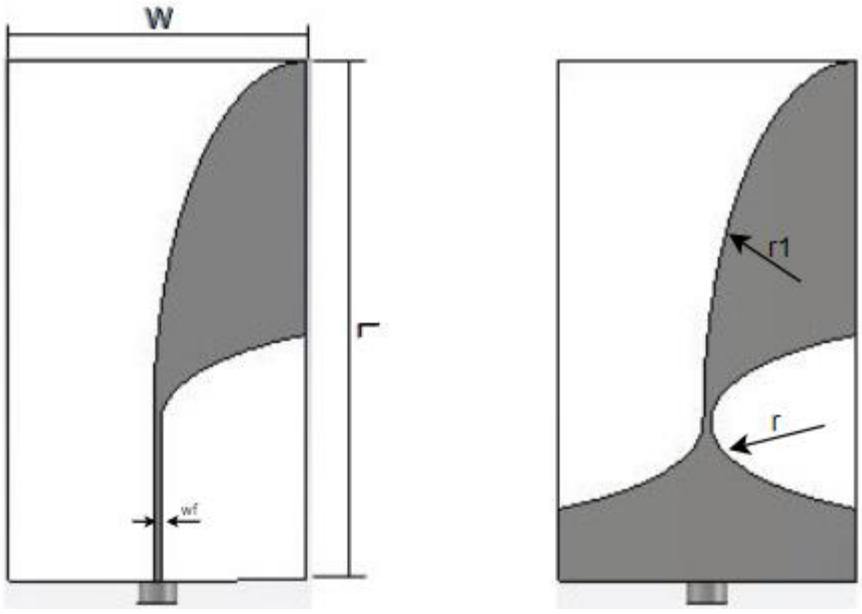

Figure 5.2: Initial Design of AVA

The antenna design shown in Figure 5.2 is designed using the mentioned information about AVA in section 3.1 and 3.3.2 and the figure shows the front side and back side of the antenna from left to right respectively. This design still needs to be improved since it does not meet the goal of this study because the UWB antennas have a band width much wider than this antenna band width which is shown in Figure 5.3. However, the substrate used for this design is FR-4 with permittivity and conductivity equal to 4.3 and 0.3 respectively and height 1.6 mm. Table 5.1 illustrates the geometry parameters.

Table 5.1: Antenna Dimensions

Parameter	Length (mm)
L	70
W	40
R	35
r1	17.5
Wf	1

The curved parts are designed using elliptic shape for simplicity and r and r1 are the x-axis and y-axis radius respectively. Elliptic curve r is in horizontal position and centered at (40, -13) and the other curve r1 the elliptic curve is vertically placed with its center location at (20, -13).

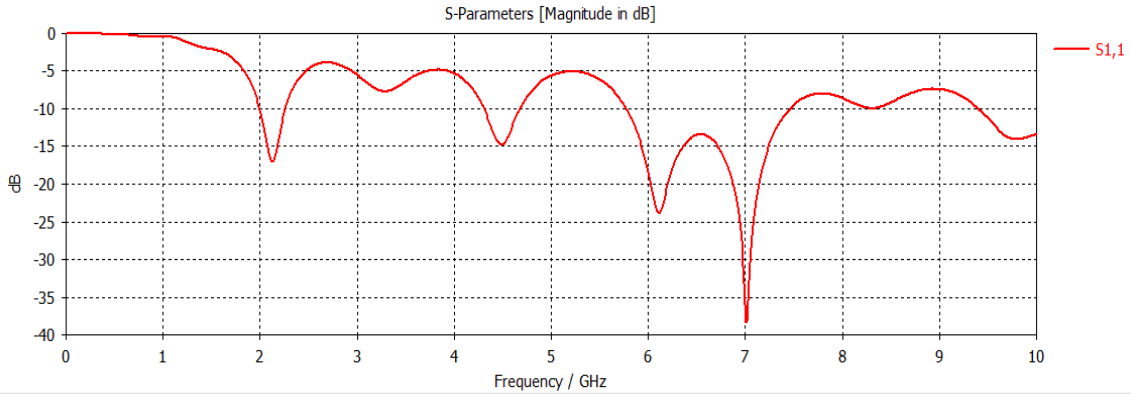

Figure 5.3: S11 for The Initial Design in Free Space

In this step of the design, the proposed antenna radiation patterns are described in section 5.3.2 at different frequencies 5GHz, 6GHz and 7GHz. It can be seen that the antenna has very high side lobe levels and this issue needs to be improved firstly in parallel to improve the main beam magnitude and the band width.

Optimization of antenna's parameters and simulation carried out in CST and slot tapered edges were used to attenuate the sidelobe level (SLL). It works to inhibit the current flow at the edges. As a result of this blocking of the current at the edges the new geometry for the modified antenna is presented in Figure5.4. However, with small optimization for antenna length next to the tapered slot edge also improves the band width. This is described in section 5.3.1, the length is reduced by 10mm and wf is changed to 2 mm, the new modified antenna is named as Palm Tree antenna.

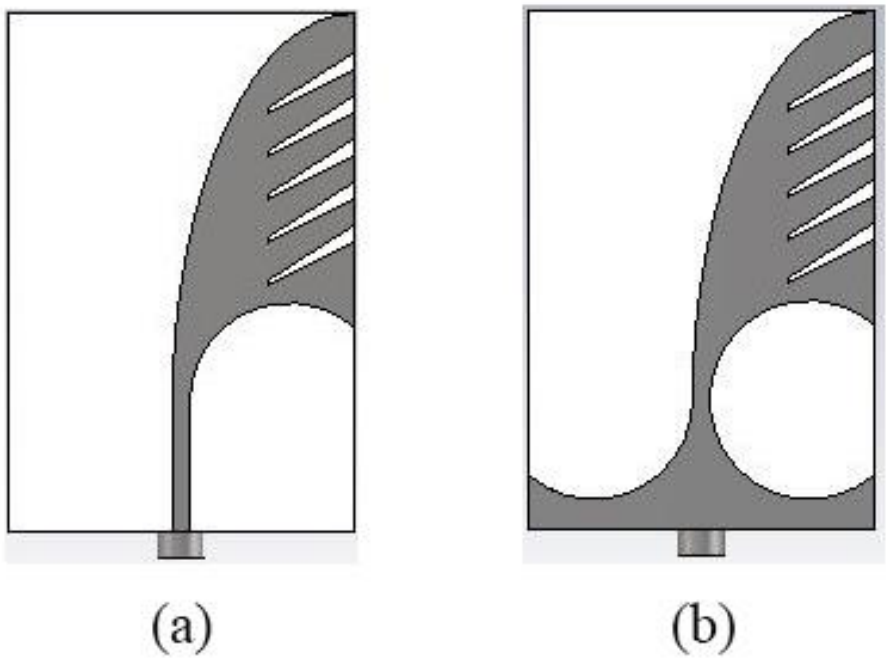

Figure 5.4: Final Designed Antenna: (a) Front Side (b) Back Side

SubMiniature version A (SAM) connector is used in this design as shown in both Figures 5.2 and 5.5 is the cylindrical part at the bottom of the antenna.

5.2 Breast and Tumor model

Breast phantom consists of two layers and has a shape of a hemisphere; in this study these layers are skin and fat. The phantom is designed using CST microwave studio features by creating biological materials shown in Figure 5.5 which has a central radius of 50 mm and top radius of 10 mm and the skin layer has a thickness of 2 mm. The electrical properties of each layer are tabulated in Table 5.2.

Table 5.2: Electric Property of Breast Phantom.

Material	Permittivity	Conductivity (S/m)
Skin	9	0.4
Fat	5.15	0.514
Tumor	54.9	4

Moreover, the tumor model has a shape of a sphere with various diameters as 10 mm, 7 mm and 5 mm and the phantoms are shown in Figures 5.2 and 5.3 for healthy and cancerous phantom respectively.

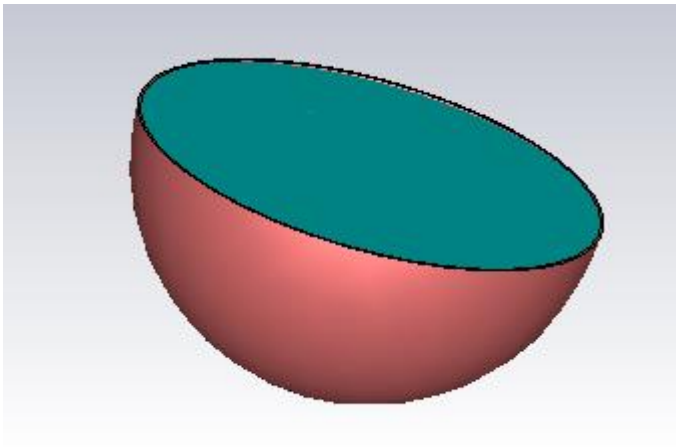

Figure 5.5: Breast Phantom

5.3 Parameter Characterization

In this section the designed antenna performance characteristics are illustrated using CST microwave studio 2020 version.

5.3.1 Return Loss (S11) and VSWR

S11 is the symbol for the reflection coefficient and it is also called as return loss which indicates the amount of reflected power usually measured in decibel scale, moreover -10 dB is the reference point which means that the third of the power is transmitted. Figure 5.3 represents the S11 plot for the initial design of the antenna which has a band from 5.78GHz to 7.47GHz.

After applying the tapered slot edges technique to the modified antenna the new S11 plot is present in Figure 5.7 as a solid line and it highlights the minimum S11 that the antenna has -48dB at 9.2GHz and has a wide bandwidth starting from 3.38GHz, while the dashed line shows the first design behavior.

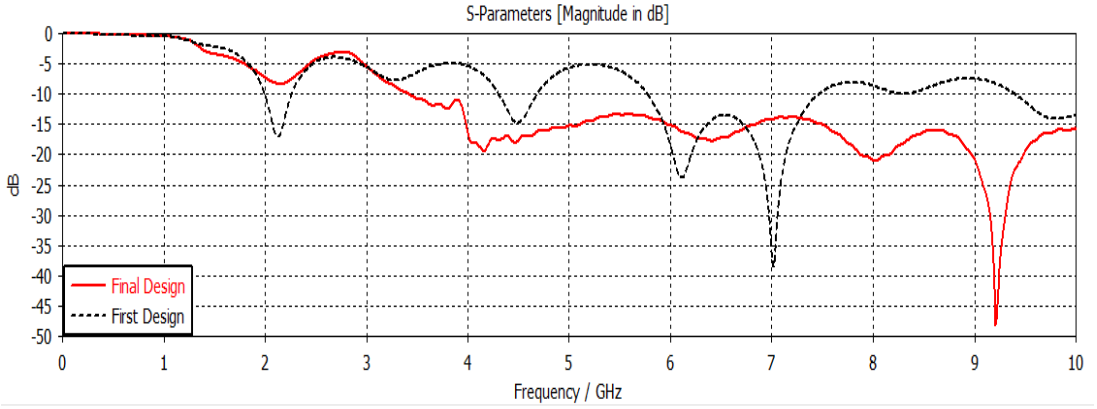

Figure 5.6: S11 for The First and The Final Design

Also, the VSWR for the final designed antenna is represented in figure 5.8 and it shows that the VSWR is less than 2 over the operating frequency.

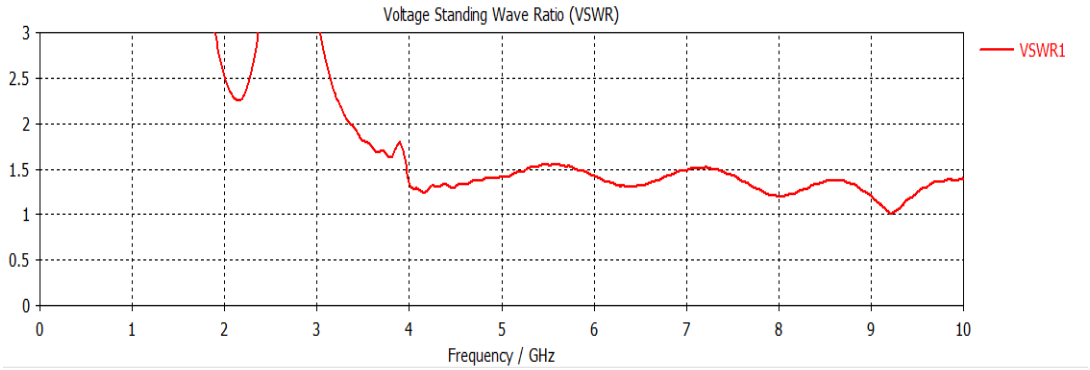

Figure 5.7: Voltage Standing Wave Ratio (VSWR)

The S11 when the healthy breast phantom is presented is shown in Figure 5.8.

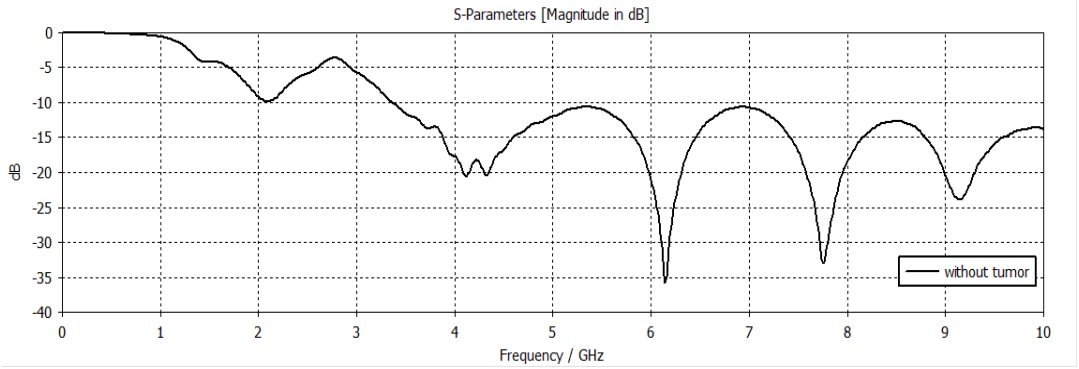

Figure 5.8: The S11 for The Healthy Breast Phantom

However, in Figure 5.8 S11 the minimum frequency is at 6.18 GHz. It is better to study the effect of return loss at that frequency since it can be used as a tool to classify whether the breast phantom is healthy or has become a cancerous cell. In the case of a tumor the S11 will be different and the great reflection happening in Figure 5.9 represents the scattered field for the breast phantom status with and without tumor.

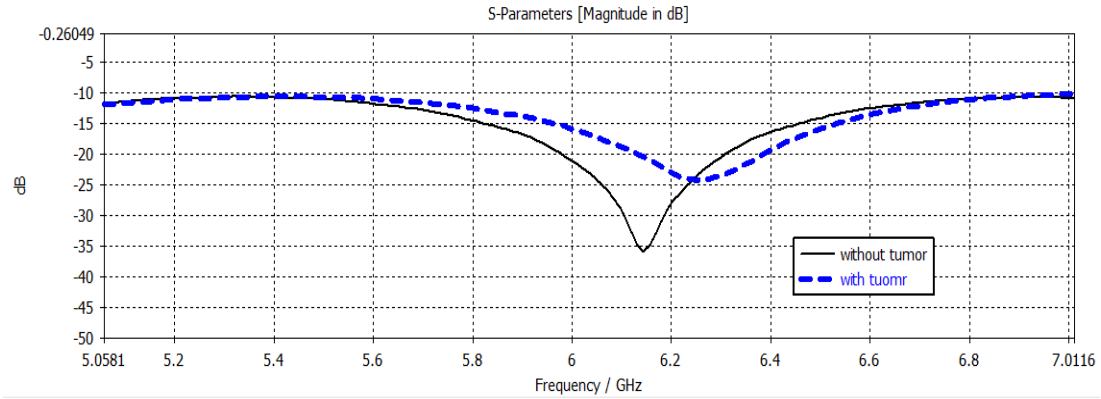

Figure 5.9: S11 for Breast with and Without Tumor

The dashed line in Figure 5.9 shows the S11 where the tumor is present and there is 10 dB more in reflection from -35 dB to -25 dB and slight shift to the right.

5.3.2 Radiation Pattern

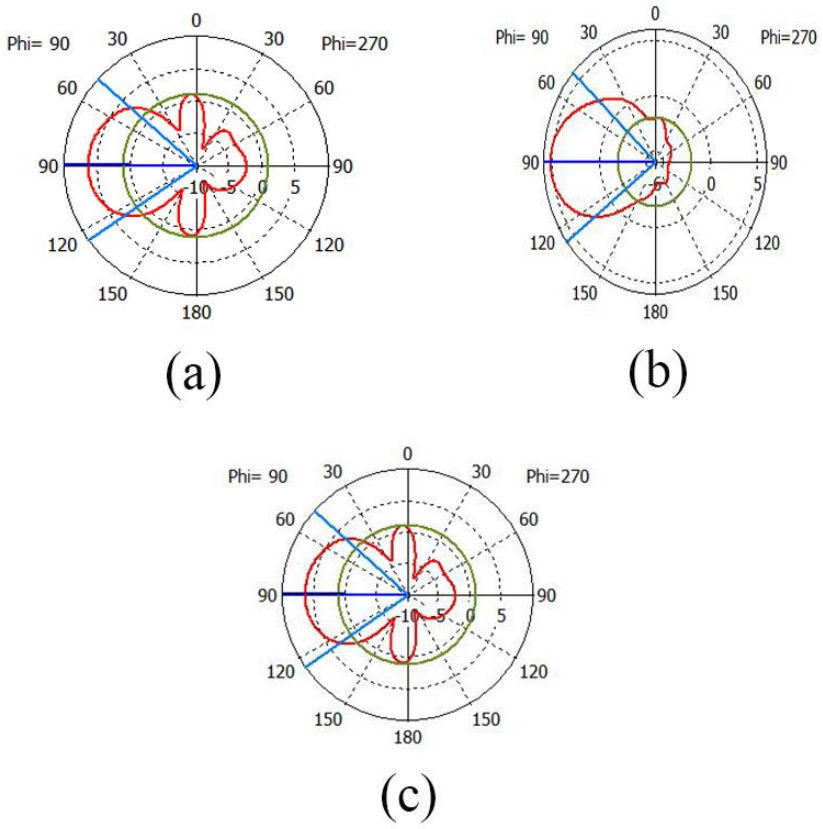

Figure 5.10: Radiation Pattern for Initial Design: (a) at 5 GHz, (b) at 6 GHz and (c) at 7 GHz

Figure 5.10 (a), (b) and (c) show the antenna radiation patterns at frequencies 5 GHz, 6 GHz and 7 GHz respectively. The main lobe magnitude in Figure 5.10 (a) representing the directivity of the antenna is 5.07 dBi while the beamwidth is 112.5 degree and SLL is -6.1 dB. In Figure 5.10 (b) the main lobe magnitude is 5.81 dBi, 79.9 degree is the beamwidth and -7.1 dB is the side lobe level; in Figure 5.10 (c) these values are 6.21 dBi, 77.7 degree and -5.2 dB.

However, from the results mentioned above the antenna has high side lobe level and the beam width still needs improvement to reach 125 degree.

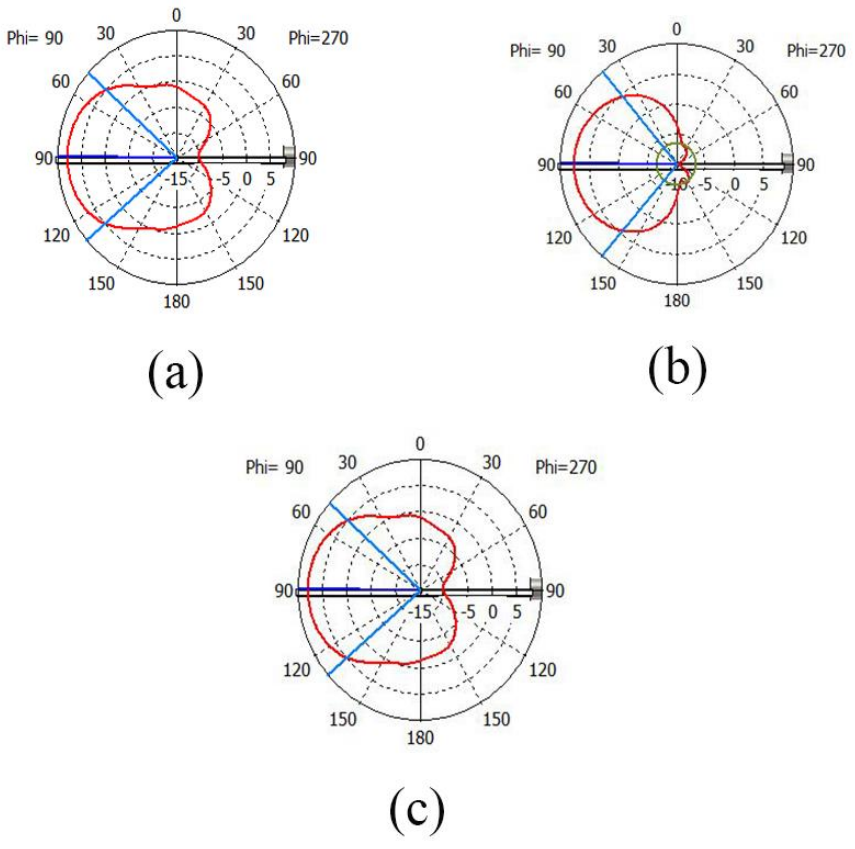

Figure 5.11: Modified Antenna Radiation Patterns at: (a) 5GHz, (b) 6GHz and (c) 7GHz

Figure 5.11 (a), (b) and (c) show the modified antenna with TSE radiation patterns at specific chosen frequencies 5GHz, 6GHz and 7GHz respectively. The antenna side lobe levels are improved after using tapered slot edges, at 5GHz the main lobe magnitude representing the directivity is increased to 6.57dBi and the beamwidth also became wider to 123.6 degree, moreover the side lobe level is improved to -18.8dB.

At 6GHz, beamwidth is 100.1 degree, directivity is 7.46dBi and side lobe level is -13.9dB; at 7GHz shown in Figure 5.11 (c) directivity is 7.81dBi, beam width 82.9 and no side lobes.

5.3.3 Specific Absorption Rate (SAR)

The human body absorption amount of electromagnetic waves is the definition of the specific absorption rate and it can be calculated using equation 5.3.

$$SAR = \frac{\sigma |E|^2}{\rho} \tag{5.3}$$

where E is the electric field (V/m), σ is tissue conductivity (S/m) and ρ is tissue mass density (Kg/m3).

Malignant tissues have high dielectric properties than the normal tissues, therefore, the SAR values which indicates the place where this absorption is maximum which is the tumor location due to the high absorption by malignant tissues because of the difference in dielectric properties between the tissues.

Several tests have been done to calculate the maximum value of SAR. The tumor has a spherical shape with a radius of 10 mm in the first test then is changed to 7mm and 5mm. For the three tests, the antenna position is changed to three different places: close to the tumor, far from the tumor and beside the tumor.

IEEE C95.1-1999 and IEEE C95.1-1999 standards require a limitation for SAR to be not harmful for human body. In this study the scale 10g is used and SAR must be less than 2 W/Kg [28],[29]; for safety, the antenna is shifted 4cm from the breast phantom and the SAR value for a healthy breast without the tumor is illustrated in Table 5.3.

Table 5.3: SAR for Healthy Breast

Frequency	SAR (W/Kg)
5GHz	1.39
6GHz	1.8
7GHz	1.73
8GHZ	1.63

Tumor and antenna locations are illustrated in Figure 5.12 and Figure 5.13.

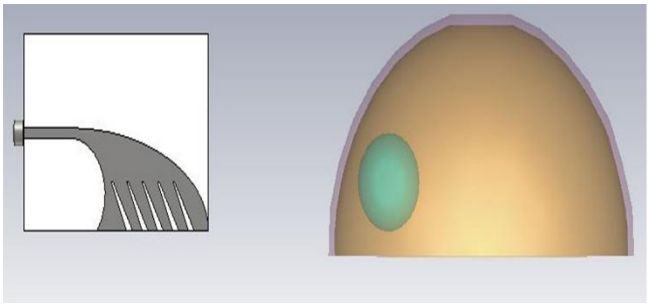

Figure 5.12: Side View for the Setup in CST

Figure 5.13 (a), (b) and (c) show the antenna location (47, -2.5,8), (-95, -3,8) and (-22,65,20) respectively, these coordinates are the center point for the aperture slot of the antenna, while the tumor is placed at (0,0,0) as the center point of the sphere.

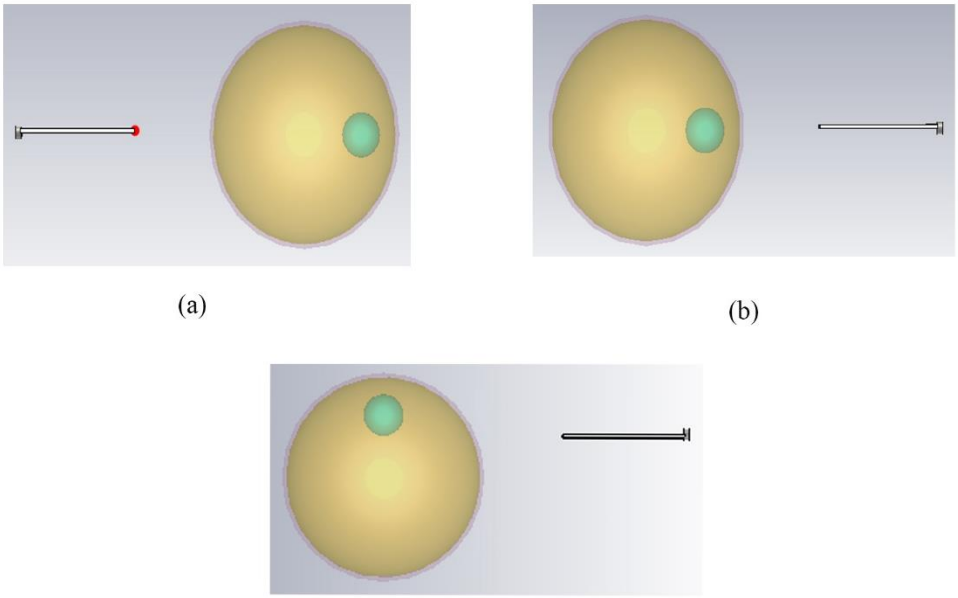

Figure 5.13: Three Different Places for Antenna

Figure 5.14 shows the tumor highlighted in red which means the SAR is maximum in that place; Tables 5.4, 5.5 and 5.6 summarize all the results of the tests.

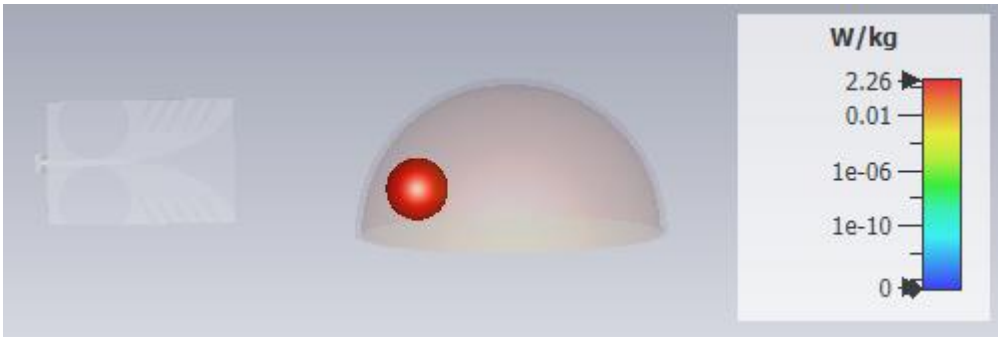

Figure 5.14: SAR at Tumor

The outer shell for the sphere which is facing the antenna is supposed to absorb more because the radiation of electromagnetic waves is from that side therefore the maximum outer point from each side must be noted and it changes by the radius.

Table 5.4: SAR Maximum Loction for Tumor of Raduis 10 mm.

Tumor reference central point (0,0,0)		
antenna position	**5 GHz**	**6 GHz**
(47,-2.5,8)	(8.7413, -3.368, 2.36659)	(9.40, -2.86, 0.359)
(-95,-3,8)	(-73.72, -1.69, -13.87)	(-73.72, -1.69, -13.87)
(-22,65,20)	(-24.89, 35.60, 5.95)	(-24.89, 35.60, 5.95)
antenna position	**7 GHZ**	**8 GHz**
(-125,-18,-16)	(9.409, -3.368, 0.359)	(9.40, -3.368, 0.359)
(-95,-3,8)	(-73.72, -1.69, -13.87)	(-73.72, -1.69, -13.87)
(-22,65,20)	(-24.89, 35.60, 5.95)	(-24.89, 35.60, 5.95)

Table 5.5: SAR Maximum Loction for Tumor of Raduis 7 mm.

Tumor reference central point (0,0,0)		
antenna position	**5 GHz**	**6 GHz**
(47,-2.5,8)	(9.435, -3.368, 1.028)	(9.435, -3.368, 1.028)
(-95,-3,8)	(-73.72, -1.69, -13.87)	(-73.72, -1.69, -13.87)
(-56,-108,-16)	(-46.7, -65.52, -40.3)	(-46.7, -65.52, -40.3)
antenna position	**7 GHZ**	**8 GHz**
(47,-2.5,8)	(9.435, -3.368, 1.028)	(9.435, -2.869, 1.028)
(-95,-3,8)	(-73.72, -1.69, -13.87)	(-73.72, -1.69, -13.87)
(-22,65,20)	(-24.89, 35.60, 5.95)	(-24.89, 35.60, 5.95)

Table 5.6: SAR Maximum Loction for Tumor of Raduis 5 mm.

Tumor reference central point (0,0,0)		
antenna position	**5 GHz**	**6 GHz**
(47,-2.5,8)	(9.144, -3.368, 2.366)	(17.341, -1.69, -13.8706)
(-95,-3,8)	(-73.72, -1.69, -13.87)	(-73.72, -1.69, -13.87)
(-56,-108,-16)	(-46.7, -65.52, -40.3)	(-46.7, -65.52, -40.3)
antenna position	**7 GHZ**	**8 GHz**
(-125,-18,-16)	(17.341, -1.69, -13.87)	(9.144, -1.69, 1.028)
(-95,-3,8)	(-73.72, -1.69, -13.87)	(-73.72, -1.69, -13.87)
(-22,65,20)	(-46.7, -65.52, -40.3)	(-46.7, -65.52, -40.3)

The tumor location inside the breast is successfully investigated using the SAR analysis feature provided by CST at different frequencies while the antenna is facing the tumor.

Chapter 6

CONCLUSION

Design of antipodal Vivaldi antenna is presented in this thesis and side lobe level (SLL) and the antenna directivity both are improved by applying tapered slot edge (TSE); the new design can be named as Palm Tree antenna. The study is carried out by CST microwave studio 2020 version.

As the simulation results show side lobe levels are -18.8 and -13.9 at 5 GHz, 6 GHz respectively and at 7 GHZ it doesn't have any sidelobes moreover the directivity is equal to 6.57, 7.46, 7.81dBi at 5 GHz, 6 GHz and 7 GHz respectively; moreover, a wide band operating frequency is achieved from 3.38 to 10GHZ.

Tumor location inside the breast model is successfully obtained by investigating the location where the SAR is maximum due the high conductivity of the malignant tissues the absorption is also high. The tumor having a spherical shape is used with radii from 10mm, 7mm to 5mm and randomly centered at (0, 0, 0) inside the breast; the results show the correct tumor location while the antenna is facing the tumor. The result at (9.435, -2.869, 1.028) shows the max SAR at 8GHz for tumor with a radius of 7mm the absorption for EM waves starting from the outer shell of the sphere; in this case the antenna was on the right of the sphere. The shell surface centered at (9.40, -2.86, 0.359) is the position of maximum SAR.

REFERENCES

[1] C. DeSantis, R. Siegel, and A. Jemal, "Breast cancer facts and figures 2013-2014," *American Cancer Society*, vol. 2013, pp. 1-38, 2013.

[2] J. V. Frangioni, "New technologies for human cancer imaging," *Journal of clinical oncology*, vol. 26, no. 24, p. 4012, 2008.

[3] S. Adnan, "Ultra-wideband antenna design for microwave imaging applications. Design, optimisation and development of ultra-wideband antennas for microwave near-field sensing tools, and study the matching and radiation purity of these antennas within near field environment," University of Bradford, 2013.

[4] Y. Lu, K. S. Yeo, A. Cabuk, J. Ma, M. A. Do, and Z. Lu, "A novel CMOS low-noise amplifier design for 3.1-to 10.6-GHz ultra-wide-band wireless receivers," *IEEE Transactions on Circuits and Systems I: Regular Papers*, vol. 53, no. 8, pp. 1683-1692, 2006.

[5] C. Peixeiro, "Microstrip patch antennas: An historical perspective of the development," in *2011 SBMO/IEEE MTT-S International Microwave and Optoelectronics Conference (IMOC 2011)*, 2011: IEEE, pp. 684-688.

[6] R. Mishra, "An overview of microstrip antenna," HCTL Open International Journal of Technology Innovations and Research (IJTIR), vol. 21, no. 2, 2016.

[7] D. Guha and Y. M. Antar, Microstrip and printed antennas: new trends, techniques and applications. John Wiley & Sons, 2011.

[8] R. Garg, P. Bhartia, I. J. Bahl, and A. Ittipiboon, *Microstrip antenna design handbook*. Artech house, 2001.

[9] R. Janaswamy, Radiowave propagation and smart antennas for wireless communications. Springer Science & Business Media, 2001.

[10] W. L. Stutzman and G. A. Thiele, *Antenna theory and design*. John Wiley & Sons, 2012.

[11] C. A. Balanis, *Antenna theory: analysis and design*. John wiley & sons, 2016.

[12] P. Gibson, "The vivaldi aerial," in *1979 9th European Microwave Conference*, 1979: IEEE, pp. 101-105.

[13] K. Ebnabbasi, D. Busuioc, R. Birken, and M. Wang, "Taper design of Vivaldi and co-planar tapered slot antenna (TSA) by Chebyshev transformer," *IEEE transactions on antennas and propagation*, vol. 60, no. 5, pp. 2252-2259, 2012.

[14] S. Ramesh and T. R. Rao, "High Gain Dielectric Loaded Exponentially Tapered Slot Antenna Based on Substrate Integrated Waveguide for V-Band Wireless Communications," *Applied Computational Electromagnetics Society Journal*, vol. 29, no. 11, 2014.

[15] T.-G. Ma and S.-K. Jeng, "Planar miniature tapered-slot-fed annular slot antennas for ultrawide-band radios," *IEEE transactions on Antennas and Propagation*, vol. 53, no. 3, pp. 1194-1202, 2005.

[16] R. Rajaraman, "Design of a wideband Vivaldi antenna array for the snow radar," *Master's thesis, The University of Kansas, India*, 2004.

[17] J. P. Weem, Z. Popovic, and B. M. Notaros, "Vivaldi antenna arrays for SKA," in IEEE Antennas and Propagation Society International Symposium. Transmitting Waves of Progress to the Next Millennium. 2000 Digest. Held in conjunction with: USNC/URSI National Radio Science Meeting (C, 2000, vol. 1: IEEE, pp. 174-177.

[18] J. B. Knorr, "Slot-line transitions (short papers)," *IEEE transactions on Microwave Theory and Techniques*, vol. 22, no. 5, pp. 548-554, 1974.

[19] S. A. AbdelBaky and H. F. Hammad, "Modified elliptical antipodal Vivaldi antenna with elliptical tapered slot edge and circular loads," in *2017 International Workshop on Antenna Technology: Small Antennas, Innovative Structures, and Applications (iWAT)*, 2017: IEEE, pp. 199-202.

[20] J. Noronha, T. Bielawa, C. R. Anderson, D. G. Sweeney, S. Licul, and W. A. Davis, "Designing Antennas For UWB Systems," *Microwaves & RF*, vol. 42, no. 6, pp. 53-54, 2003.

[21] C. R. UK. https://www.cancerresearchuk.org/about-us (accessed 22 May, 2020).

[22] T. England, "Dielectric properties of the human body for wave-lengths in the 1–10 cm. range," *Nature*, vol. 166, no. 4220, pp. 480-481, 1950.

[23] T. England and N. Sharples, "Dielectric properties of the human body in the microwave region of the spectrum," *Nature*, vol. 163, no. 4143, pp. 487-488, 1949.

[24] M. S. Banu, S. Vanaja, and S. Poonguzhali, "UWB microwave detection of breast cancer using SAR," in *2013 International Conference on Energy Efficient Technologies for Sustainability*, 2013: IEEE, pp. 113-118.

[25] D. Watmough and K. Quan, "X-ray mammography and breast compression," *Lancet (British edition)*, vol. 340, no. 8811, 1992.

[26] S. C. Bushong, Diagnostic Ultrasound: Essentials of Medical Imaging Series. McGraw-Hill/Appleton & Lange, 1999.

[27] M. H. o. T. County, 2020. [Online]. Available: http://www.mhtcguymon.org/.

[28] D. Seabury, "An update on SAR standards and the basic requirements for SAR assessment," *Feature Article, Conformity*, pp. 1-8, 2005.

[29] J. C. Lin, "A new IEEE standard for safety levels with respect to human exposure to radio-frequency radiation," *IEEE Antennas and Propagation Magazine*, vol. 48, no. 1, pp. 157-159, 2006.